ELSEVIER

Polymer 42 (2001) 3609–3625

polymer

www.elsevier.nl/locate/polymer

Chemical and physical modifications of alternating ethylene–carbon monoxide copolymer by outdoor exposure

F. Severini[a,*], R. Gallo[b], L. Di Landro[a], M. Pegoraro[a], L. Brambilla[a], M. Tommasini[a], C. Castiglioni[a], G. Zerbi[a]

[a]*Dipartimento di Chimica Industriale e Ingegneria Chimica del Politecnico di Milano, Piazza Leonardo da Vinci, 32 20133 Milano, Italy*
[b]*Dipartimento di Chimica Industriale, Università di Messina, 98100 Messina, Italy*

Received 10 July 2000; received in revised form 30 August 2000; accepted 25 September 2000

Abstract

Infrared and Raman spectroscopy, thermal analysis, electron scanning microscopy and mechanical tests have been performed to study the outdoor ageing of Carilon (a terpolymer which can be described as an ethylene–carbon monoxide alternate copolymer containing a small amount of propylene units).

The results of these analysis are discussed and compared to obtain a description of the structural modifications induced by photodegradation. All the experiments performed show evidence of relevant structural changes in the material localised on the surface of the samples: chemical modification of the polymers, breaking of polymer chains and rearrangement of the crystalline phase can be clearly identified. Moreover, mechanical tests reveal that outdoor ageing involves to some extent the bulk of the material, with a consequent loss of mechanical properties.

Keywords: Photodegradation; Polyketones; Infrared spectroscopy

1. Introduction

In this work we focus on a polymeric material, known as Carilon, recently commercialised by Shell International Chemicals [1]. Carilon belongs to the polyketones family (POK): it is a terpolymer (POK-C2/C3) obtained by incorporating a small amount of propylene units in an alternating copolymer of ethene and carbon monoxide (POK-C2).

POK polymers are semicrystalline materials and show good mechanical properties [1] and excellent chemical stability to fuels. Effects of UV irradiation in nitrogen atmosphere of random ethylene–carbon monoxide copolymers have been described in the literature [2,3]. Only some general information [4] can be found about the photochemical degradation of copolymers with different carbon monoxide content; however, systematic studies on the outdoor ageing of these materials did not so far appear in the literature.

Here we present a systematic study of the effects induced by outdoor exposure on Carilon plates, for a very wide range of exposure times and analysed with several different techniques.

This work follows a previous study by the same authors on the outdoor ageing of thin films of the same material [5].

2. Experimental

A general-purpose injection grade 'Carilon Polymer D 26 HM100' has been used as received from Shell Italia Spa. Sheets with 1 mm thickness were obtained by compression moulding polymer granules for 6 min at 225°C at 5.4 MPa pressure. Translucent plates were obtained which allowed the transmission of consistent amount of visible light through the thickness. The sheets were mounted unstressed on wooden frames tilted at 45° with respect to the horizontal plane and were exposed facing south-west on a terrace at about 20 m above ground at Messina, Italy (38° 11′ 20″ north; 15° 33′ 30″ east). The exposure started in March 1999 and lasted 8700 h up to March 2000. The spring/summer 1999 seasons during exposure, in the South of Italy, has been particularly warm and dry. In Fig. 1 the minimum and maximum temperatures observed during the exposure [6] are shown.

Thermal analyses, infrared (IR) and Raman spectroscopy,

* Corresponding author. Tel.: +39-02-2399-3227; fax: +39-02-7063-8173.
E-mail address: febo.severini@polimi.it (F. Severini).

0032-3861/01/$ - see front matter
PII: S0032-3861(00)00740-0

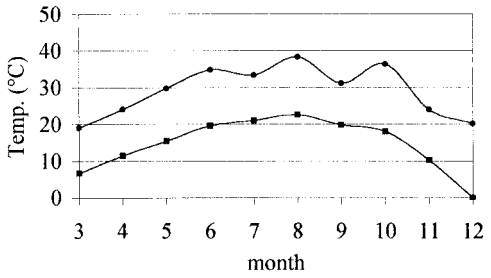

Fig. 1. Minimum and maximum temperatures (from March to December 1999) recorded in Messina (Italy).

scanning electron microscopy, mechanical tests, have been performed on samples withdrawn after different times of exposure. Some experiments (see below) were made on powders scratched from the surface of the plates by fine grinding paper. Since the scratching removes the material reaching few microns in depth, these experiments allow to investigate structural or chemical modifications confined in a region near to the surface.

DSC curves were obtained on a Perkin–Elmer DSC-2 equipped with a Perkin–Elmer 3600 Thermal Analysis Data Station. Samples of 0.8–2.6 mg were weighted into aluminium pans and heated at 20 K min^{-1} (dynamic tests). Indium was used as the standard for calibrating the temperature axis and the enthalpy output. Average deviations of the melting enthalpies are in the range of ±1%. Thermal oxidation strength was determined by thermogravimetric analysis with isothermal tests at 523 K in air. A Perkin–Elmer TGS-2 instrument was used.

The result of the measurement is expressed as the time, in minutes (with an average deviation of ±5%), required to observe the first change in the slope of the thermogravimetric curve of the sample.

IR absorption and Attenuated Total Reflection (ATR) spectra have been recorded with a Nicolet FTIR Magna 560 spectrophotometer. Spectra-Tech ATR Model 300 continuously variable equipped with a KRS5 crystal has been used for ATR experiments; the incidence angle was 50°.

Raman experiments were performed with FT-Raman Nicolet 910 spectrometer with exciting line at 1064 nm. (Nd:Yag laser). IR spectra were recorded with 1 cm^{-1} resolution; Raman spectra with 4 cm^{-1} resolution. Temperature dependent IR spectra have been recorded, using the hot stage Mettler FP800ht.

Torsional dynamic mechanical analyses of Carilon samples were performed by a Rheometrics RDAII Spectrometer at 1 Hz frequency, in a temperature range between −130°C and 230°C. Prismatic samples 1 mm × 10 mm × 35 mm cut directly from the exposed sheets were used.

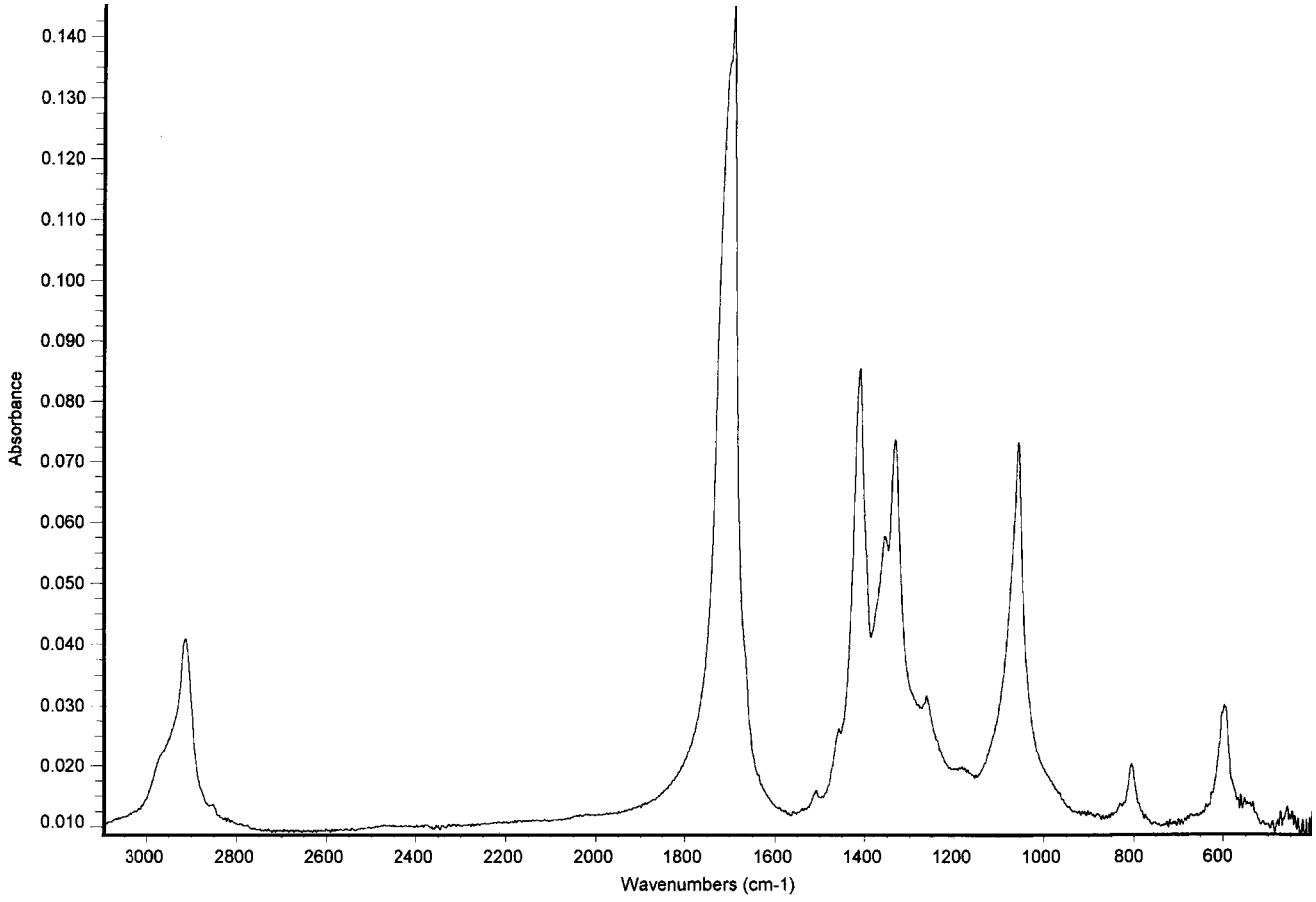

Fig. 2. FT-IR spectrum of pristine Carilon (Powder from a plate, in KBr pellet).

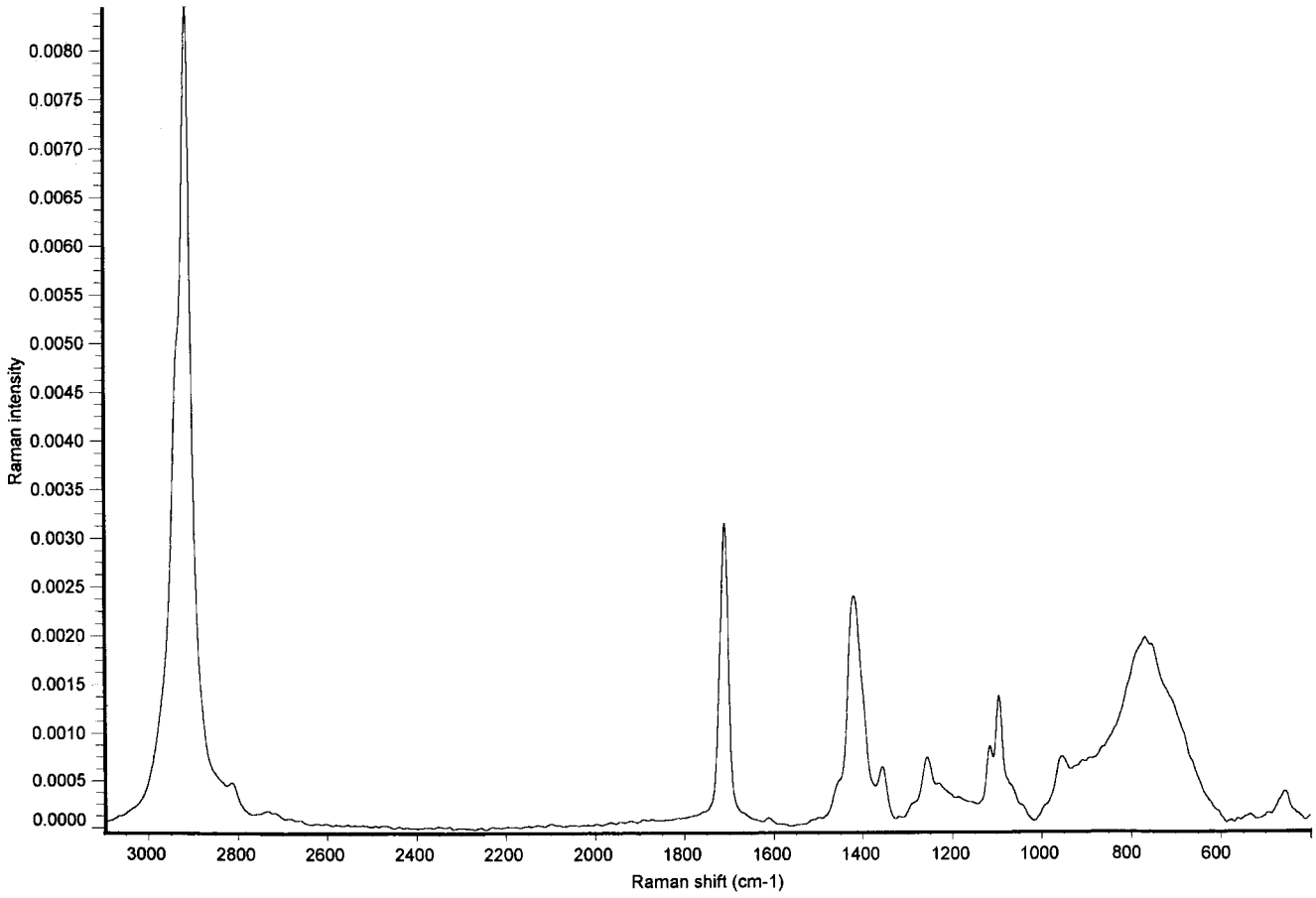

Fig. 3. FT-Raman spectrum (λ_{exc} = 1064 nm) of a sample of pristine Carilon. Sample was a plate.

Tensile tests were performed according to ASTM D638 (type III specimens) by an Instron 4302 dynamometer at 10 mm/min cross-head rate. Approximate values of strain at break were determined as ratio of the cross-head displacement to the estimated gauge length.

The surface morphology was observed by a Zeiss 940 Digital Scanning Electron Microscope (SEM). Sample sections were observed after fracture in liquid nitrogen.

3. Infrared and Raman spectra of Carilon samples

The structure of perfectly alternating copolymer of ethylene and carbon monoxide (POK/C2) and terpolymers (POK-C2/C3) obtained by incorporating a small amount of propylene units in the polymer backbone, have been already reported [7,8]. According to X-rays diffraction analysis performed on POK/C2 [8] two crystalline modifications (the α phase, stable at low temperatures and the β phase) have been identified: they are characterised by a different degree of packing in the crystal unit cell, with a higher density in the case of the α phase. The occurrence of randomly distributed methyl groups along the chain has influence on the crystal structure and on the degree of crystallinity of the samples [7]; defects along the chain hinder the formation of the most dense α phase and at above 5% propylene content the crystal phase is almost β.

Both in the α and the β phases, the crystal structures are described in terms of an orthorombic lattice, with two chains per unit cell [7,8]. The conformation of the polymer chain is the same in both crystals, showing a planar zigzag structure of the carbon backbone. A single POK/C2 chain in regular conformation is then represented by the one-dimensional translational unit:

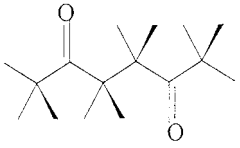

Several Carilon samples (before and after outdoor exposure) have been analysed with IR and Raman experiments. The thermal history of the pristine material and of the material after outdoor exposure have been followed by recording the IR spectra at different temperatures ranging from room temperature up to the melting of the sample.

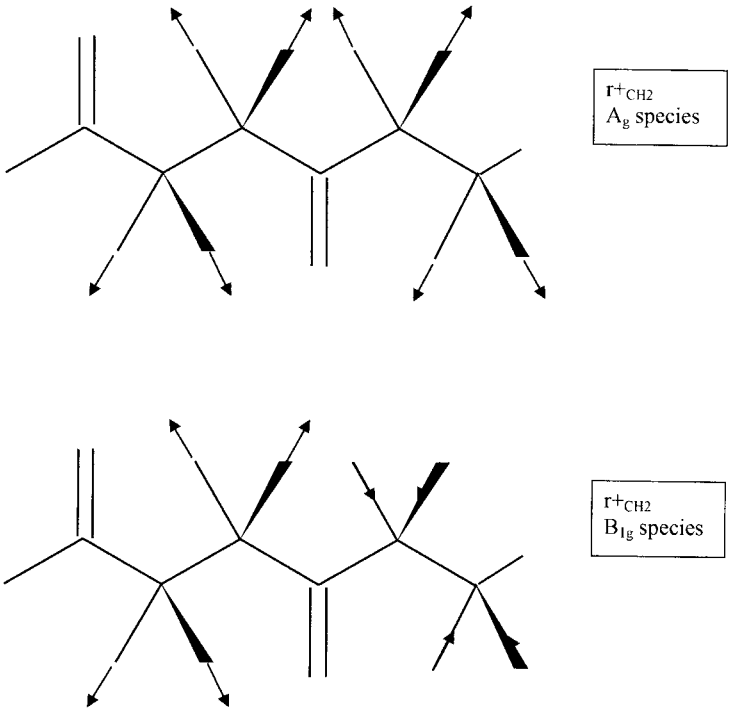

Fig. 4. Sketch of a couple of $\mathbf{k} = 0$ symmetry coordinates (symmetric CH_2 stretchings) of a regular POK/C2 chain belonging to A_g and B_{1g} symmetry species, respectively.

3.1. Infrared and Raman spectra of the pristine material (before outdoor exposure): assignment of the vibrational transitions

The Raman spectrum of a Carilon plate, has been recorded with exciting laser line $\lambda_{exc} = 1064$ nm. The IR spectra have been recorded both on a Carilon powder, obtained from the same plate and dispersed in a KBr pellet (in this way it is possible to perform absorption experiments on solid samples), and directly on the plate surface, with ATR technique.

IR and Raman spectra (Figs. 2 and 3) show a simple spectral pattern with few bands, as expected for a polymer with small and highly symmetric chemical units.

Moreover, the occurrence of chemical defects, i.e. the occurrence of propylene units in the chain, was detected by observing the characteristic IR group frequencies of the methyl group, namely a weak band at 1460 cm^{-1} assigned to a bending vibration localised on the methyl group which can be seen both in the Raman and in the IR spectrum of our sample. The assignment of this frequency can be made by correlation with the observed fundamental transition in polypropylene at 1459 cm^{-1} [9,10]; notice that the 1460 cm^{-1} Raman band has been already used as marker of the presence of propylene units in the spectra of samples at different known content of propylene units [11], since its intensity shows linear increase with the propylene content in the polymer chain. Minor features in the high frequency side of the CH stretching fundamental transitions, can be observed in the IR spectrum and assigned to CH_3 group. The melting temperature (220°C) observed on a pristine Carilon sample (see Section 5) supports our conclusion about the occurrence of a non-negligible fraction of propylene units in the polymer chains (For a discussion of the evolution of T_{melt} with propylene content in POK, see Ref. [7]).

Due to the occurrence of a sufficient amount of propylene units randomly distributed in the chains we expect that: (i) The crystalline phase in the pristine material is mainly β. (ii) An appreciable content of amorphous phase due to non-crystallisable molecules and/or to chain segments richer in propylene would exist.

Vibrational spectra of crystalline polymers can be interpreted on the basis of a structural model where the polymer chain is described as a one-dimensional crystal, i.e. as an infinite polymer chain with translational symmetry [12,13]. Indeed, interchain interactions are generally weak and can be neglected in a first approximation. The presence of a three-dimensional crystalline structure may eventually give rise to characteristic signals (crystal splittings of the fundamental bands) that are not accounted for by a one-dimensional treatment [12,13].

In this work, the fundamental transitions arising from the conformationally regular chain which belongs to the β crystal were identified and assigned according to vibrational dynamics of a one-dimensional crystal.[1]

[1] In this treatment the fact that the real material contains propylene units is obviously neglected. A relatively small amount of C3 unit can be indeed seen as "defects" which eventually give rise to deviation from the ideal behaviour predicted on the basis of one-dimensional crystals.

Table 1
Assignment of Raman and IR fundamental frequencies of Carilon. r+, r−, δ, W(CH_2), T, P, indicate symmetric and antisymmetric CH_2 stretchings, bending, wagging, twisting, rocking of methylene groups (see Ref. 12 for definitions). ω indicates C–C–C bendings with the C atom of the carbonyl group as vertex, R are C–C strechings involving a C atom of the carbonyl group, τ are torsions, opla are out-plane bendings

A_g and B_{1g}			
	Assignment	ν (cm^{-1})	
	r+(CH_2)	2915	
	δ	1426	
	W(CH_2)	1355	
A_g		B_{1g}	
Assignment	ν (cm^{-1})	Assignment	ν (cm^{-1})
str C=O	1706	str CC	1116
str CC	1095	str CC	~950
str CC	~950	W (C=O)	–
bend (CCC)	458 (or 306)	bend (CCC)	306 (or 458)
B_{2g} and B_{3g}			
	Assignment	ν (cm^{-1})	
	r−	2932	
	T	1256	
	P	755	
	τ(CC)	–	
	B_{3g}		
	Assignment	ν (cm^{-1})	
	Opla C=O	537	
B_{1u}			
	Assignment	ν (cm^{-1})	
	r−	Shoulder	
	T	1256	
	P	805	
	Opla C = O	536	
	τ (CC)	–	
B_{2u} and B_{3u}			
	Assignment	ν (cm^{-1})	
	r+	2912	
	δ	1410	
	W(CH_2)	1332	
B_{2u}		B_{3u}	
Assignment	ν (cm^{-1})	Assignment	ν (cm^{-1})
str C = O	1692		
R+	1056	R−	1056 (?)
ω+	466	ω−	466 (?)
		ω−(C=O)	601

The regular planar zigzag conformation of a POK/C2 chain is described as a 2_1 infinite helix, whose line group is isomorphous to D_{2h} symmetry point group. Normal modes of the chain are phonons characterised by a phonon wavevector **k**. Among the infinite phonons characteristic of the chain, we will observe in IR and Raman spectra those corresponding to the few allowed vibrational transitions which obey the selection rule $\mathbf{k} = 0$, that derive from translational symmetry. The number of IR and/or Raman active $\mathbf{k} = 0$ phonons can be predicted by symmetry analysis.

According to the chain structure, $\mathbf{k} = 0$ phonons can then be classified according to the symmetry species of the D_{2h} symmetry point group.

An immediate consequence on vibrational spectra derives from the fact that D_{2h} point group has the inversion symmetry operation: for this reason we predict mutual exclusion between IR and Raman transitions. If we consider experimental IR and Raman spectra (Figs. 2 and 3) we realise that this requirement is precisely fulfilled thus providing an experimental evidence of the proposed structure.

We have obtained the structure of the representation (in the vibrational space) for POK/C2 polymer at $\mathbf{k} = 0$:

$$\Gamma^{R} = 7A_g + 7B_{1g} + 4B_{2g} + 5B_{3g} + 4A_u + 5B_{1u} + 6B_{2u} + 6B_{3u}$$

Since A_g, B_{1g}, B_{2g} and B_{3g} species are Raman active; B_{1u}, B_{2u}, B_{3u} species are IR active and A_u species are inactive, we expect to see 17 fundamental bands in IR and 23 fundamental bands in the Raman.

Experimentally only 11 bands of appreciable intensity can be identified in the IR spectrum and 13 in the Raman (see Figs. 2 and 3).

This fact can be explained if $\mathbf{k} = 0$ symmetry coordinates for every symmetry species are built. In this way it is possible to see that symmetry coordinates of A_g species involving CH_2 groups describe displacements where two (CH_2–CH_2) groups separated by a carbonyl group vibrate in phase (same sign of the equivalent internal coordinates in the symmetry combination) while in the case of B_{1g} species the same group coordinates are combined with opposite sign (out of phase) as it can be seen in the example reported in Fig. 4. The same behaviour can be found if symmetry coordinates involving CH_2 groups belonging to B_{3g} and B_{2g} species (and also to B_{2u} and B_{3u} species) are compared. Since we expect a very weak dynamical interaction between internal coordinates localised, respectively on the two CH_2–CH_2 groups separated by a C=O group, we can infer that those A_g and B_{1g} normal modes which mainly involve vibrations localised on CH_2 show very close frequencies values (or perhaps accidental coincidence in frequency); obviously the same can be said for B_{3g} and B_{2g} normal modes and for B_{2u} and B_{3u} normal modes.[2]

In this way the number of different frequencies which can be identified in IR and Raman spectra is drastically reduced, as indeed it happens.

In Table 1, frequencies of the relevant transitions observed in IR and in Raman spectra are reported. Making use of symmetry analysis (see Table 1) and of classical

[2] Notice that the observed bands are broad and highly asymmetric: this behaviour reveals (see below) the presence of different solid phases and may hide the presence of more than one distinct fundamental peak with close frequency values.

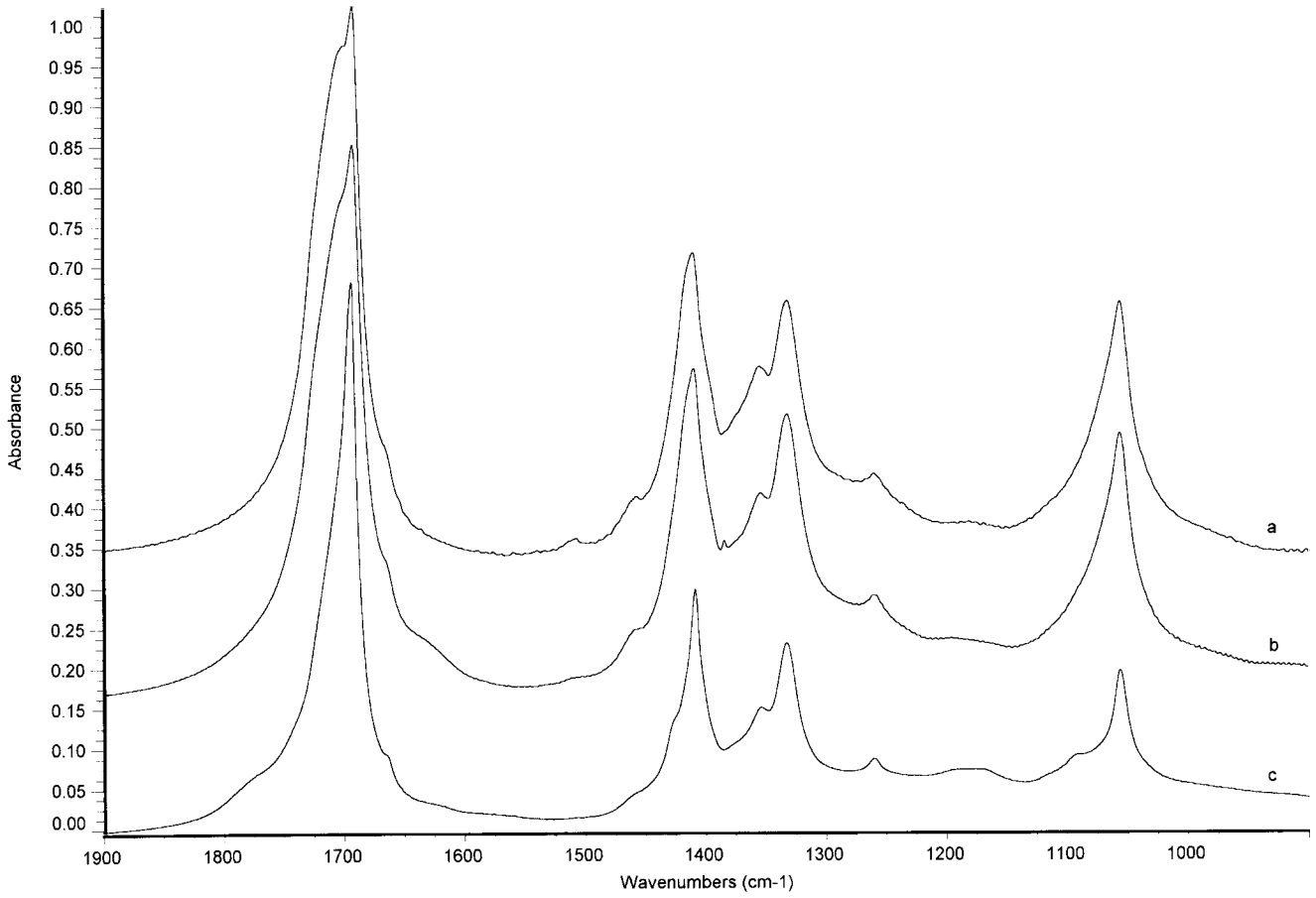

Fig. 5. IR absorption spectra of Carilon powder (in KBr pellets) obtained from surfaces of different Carilon samples: (a) Pristine unaged sample; (b) sample withdrawn after 7944 h of outdoor exposure (surface on the back); (c) sample withdrawn after 7944 h of outdoor exposure (top surface).

correlation criteria based on group frequencies [14] it is possible to suggest an assignment for all the relevant bands observed. The assignment reported in Table 1 has been made in the most cases in the hypothesis that every normal mode is characterised by a single symmetry coordinate which exhibits the largest content in the eigenvector. This hypothesis is correct only for localised vibrations: for this reason assignment of frequencies relative to the skeletal modes have been indicated with the symbol CC_{str} and/or CCC_{bend} without explicit indication of the stretching coordinates (or bending coordinates) relative to different non-equivalent CC bonds (or CCC angles).

The assignment reported in Table 1 refers to a vibrational analysis based on a model of a perfect one-dimensional crystal. However, according to the previous discussion, we expect to find some other features which arise from a disordered, amorphous phase.

At a first sight, it is very difficult to find some isolated peak which can be straightforwardly ascribed to the disordered phase. However, a better analysis of the band shapes clearly shows a common characteristic of the observed transitions: several IR and Raman bands are highly asymmetric, especially on the high frequency side, thus indicating that their complicated structures are probably due to several different components. The presence of different components is especially evident in the case of the IR C=O stretching band as it can be seen in Fig. 5(a).

These observations suggest that normal modes of chains in the disordered phase (where the disorder can be described as conformational distortion of the chain and/or due to different intermolecular environments) lie at frequencies very close to those of the regular chains packed in the three-dimensional crystal, giving rise to an envelope of bands responsible for the asymmetric shapes observed. Moreover, the crystalline phase, which is mostly β (due to the content in propylene), may contain some domains characterised by the αstructure, which also contributes with components at frequencies very close to those of the β phase.

Due to the presence of C=O, the -(CH_2–CH_2)- groups along the chain are weakly coupled. For this reason the frequencies of vibrations localised on the –(CH_2–CH_2)– units are weakly modulated by the conformation (regular, as in the crystalline phase or irregular, as in the amorphous phase) of the adjacent units along the chain. Different frequencies for different three-dimensional arrangement of the chains are also expected; however, in this case frequency shifts from one crystalline phase to the other are certainly

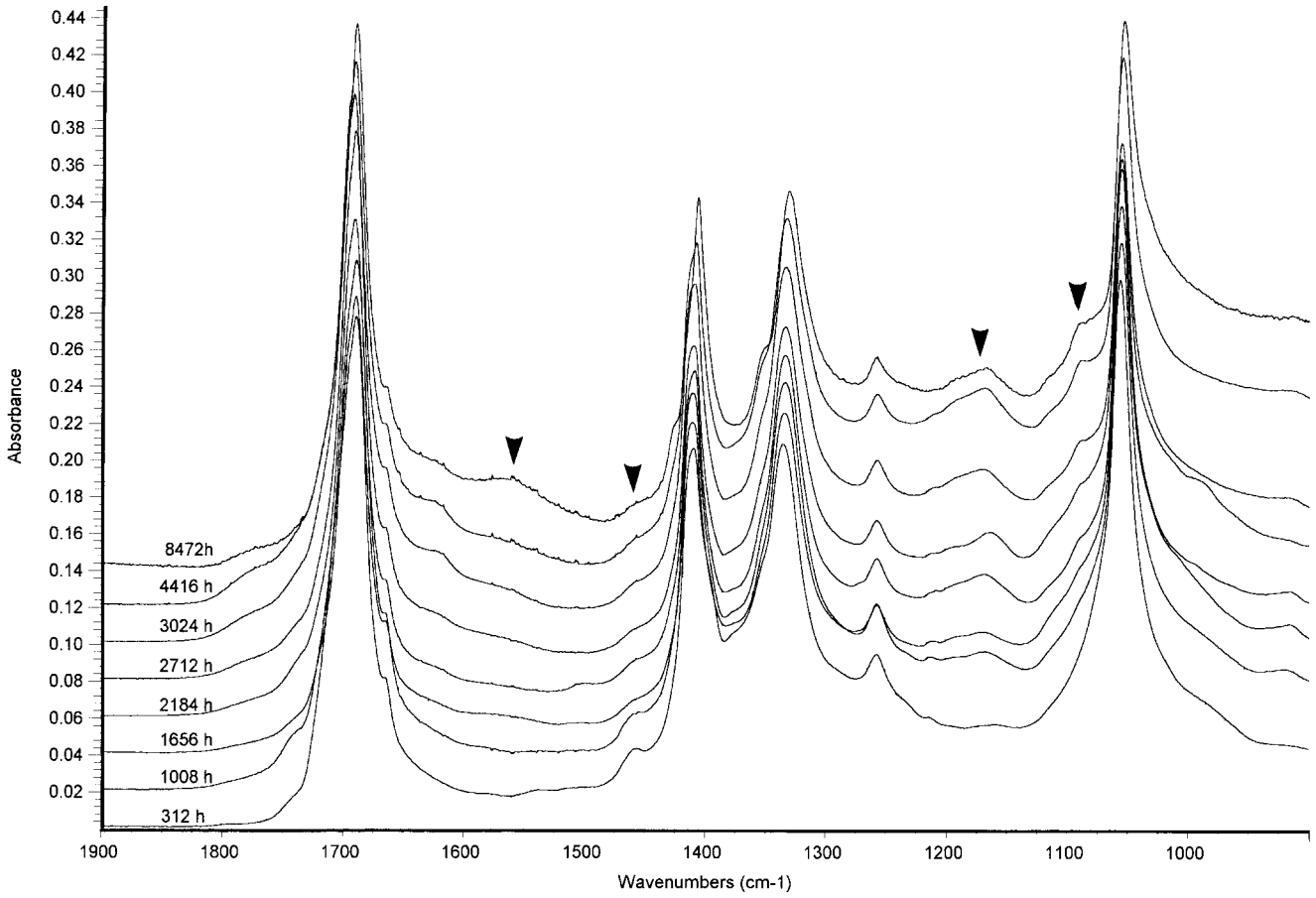

Fig. 6. ATR spectra of Carilon plates withdrawn after different times of outdoor exposure. The surfaces analysed were those directly exposed to the sun light (top surface). Arrows indicate the spectral region where changes are observed (see text).

small, since the chains conformation remains still the same both in β and in α modification.

In the case of C=O band, the large asymmetry observed can be explained in terms of relatively large frequency shifts of different components due to the presence of different dipole–dipole interactions between C=O bonds along chains in different conformations. Moreover, interactions between C=O bonds belonging to different chains, in different environments, may also give rise to components at different frequencies.

3.2. Infrared analysis of Carilon samples after outdoor exposure

We have performed IR analysis on several plates exposed for different times (from 0 up to 7944 h), in the experimental conditions described in Section 2.

All the samples were analysed by ATR technique, since due to the thickness of the plates, absorption experiments were impossible. ATR technique was used since it allows to obtain spectra of the surfaces, without any treatment or sample preparation.

From the plate withdrawn after 7944 h of exposition, two samples in the form of powder have been obtained, the first by scraping the surface directly exposed to the sun light and the second from the surface on the back. Absorbance experiments have been performed since band shape analysis is, in some cases, less reliable on ATR spectra, where several optical effects can take place.

In Fig. 6 a series of ATR spectra on the exposed surface of Carilon plates are reported. Some new features,[3] that show increasing intensity with the exposure time of the Carilon plate can be seen:

(i) A new (structured) band appears at 1167 cm^{-1}. In this spectral region stretching vibrations localised on C–O–C groups can be found (see for instance Ref. [14]). Accordingly, this band can be related to some chemical modification of the polymer with appearance of ether groups.
(ii) A shoulder at 1088 cm^{-1} and a shoulder at 1352 cm^{-1} appear after exposure. These two transitions may be assigned to fundamentals of the crystalline phase. These transitions become evident in the exposed sample since several components (e.g. those originating from amorphous

[3] These observations parallel those collected in a previous work on a series of Carilon films [5] exposed in open air in similar experimental conditions.

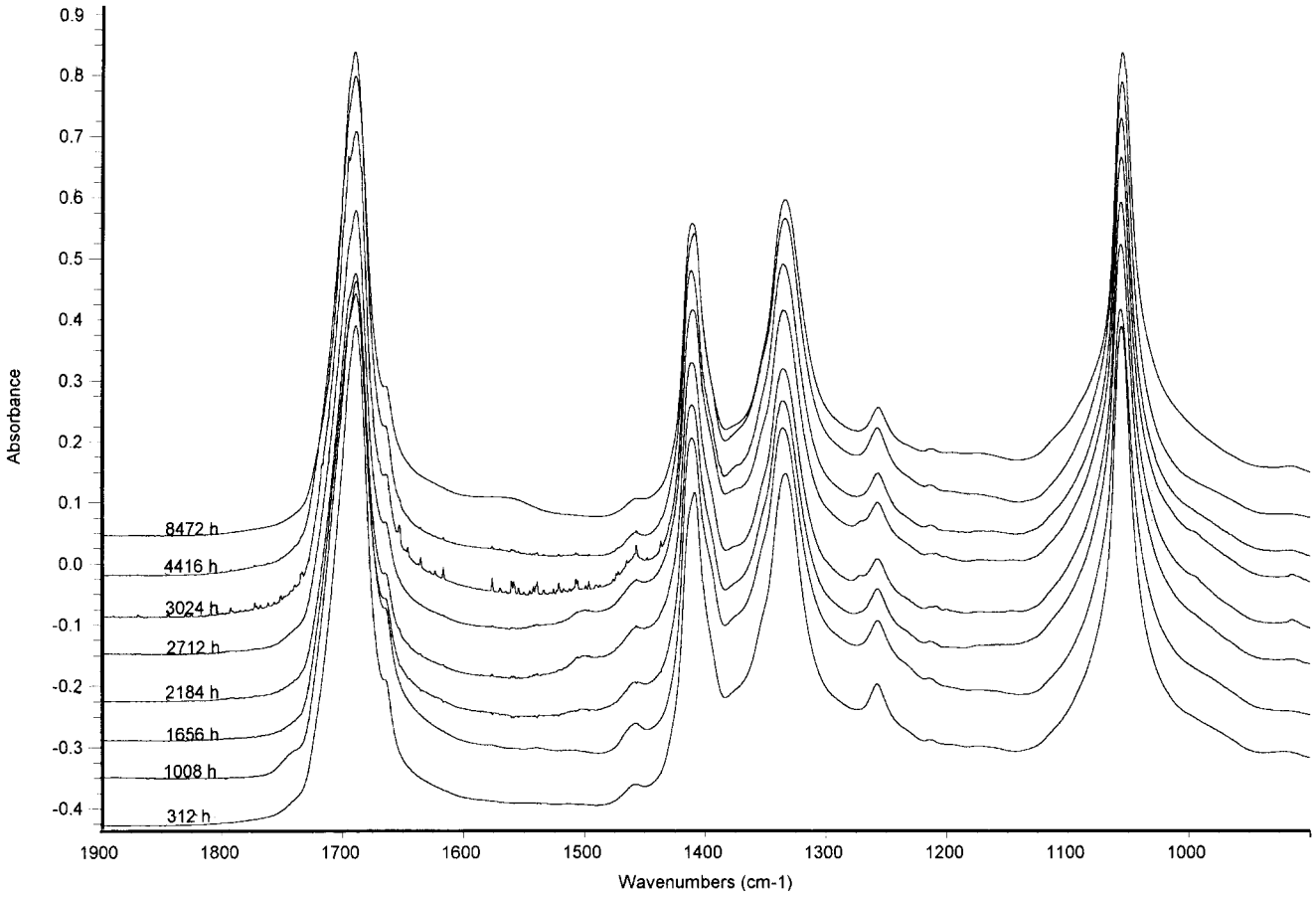

Fig. 7. ATR spectra of Carilon plates withdrawn after different times of outdoor exposure. The surfaces analysed were those not directly exposed to the sun light (surface on the back).

phase) of the closest strong bands have been 'cleaned up' by photodegradation.

(iii) After about 4000 h of exposure some weak, broad structures appear at about 1560 and 1619 cm^{-1}, probably due to formation of C=C double bonds. These same frequencies appear also in the Raman spectrum of a thermally degraded Carilon sample.

(iv) Another impressive change involves the methyl band at 1459 cm^{-1} (relative to the propylene units in the polymer chains) which practically disappears after direct exposure; also CH stretching components in the high frequency side of the CH stretching band, ascribed to methyl units, disappear.

(v) As for the band shapes, we can observe a progressive sharpening of almost all the bands: this sharpening seems to be due to the disappearance of the high frequency asymmetric components of the principal peaks. This evidence is confirmed by band shapes analysis of the two powder samples observed with absorption IR experiments.

A series of ATR spectra from the surface on the back of the same plates of Fig. 6 are reported in Fig. 7. Some evolution in the same regions as in the case of the top surfaces can be seen in this series of spectra; however, in this case the new features are very weak, thus suggesting that the direct exposure to the sun light is of fundamental importance in the degradation process.

In Fig. 5, IR absorption spectra of the two powder samples (in KBr pellet) obtained from an exposed plate are reported and compared with that of a powder sample from a plate before outdoor exposure (this spectrum is the same as that reported in Fig. 2).

The analysis of the spectra reported in Fig. 5 shows all the features observed also in ATR experiments (a broad band at 1167 cm^{-1} and a weak peak at 1088 cm^{-1} appear in the spectrum of the powder from the surface directly exposed). It is difficult to judge if a new component grows at 1352 cm^{-1}: indeed, different from the ATR spectra, absorption spectra of the pristine sample show a weak peak at this frequency.

The most important effect of the outdoor exposure which is clearly revealed by the spectra of Fig. 5 is certainly the drastic reduction of the high frequency components of all bands after exposure of the sample (compare Fig. 5(a) and (c)). Not only CH_2 deformation bands and CC stretching

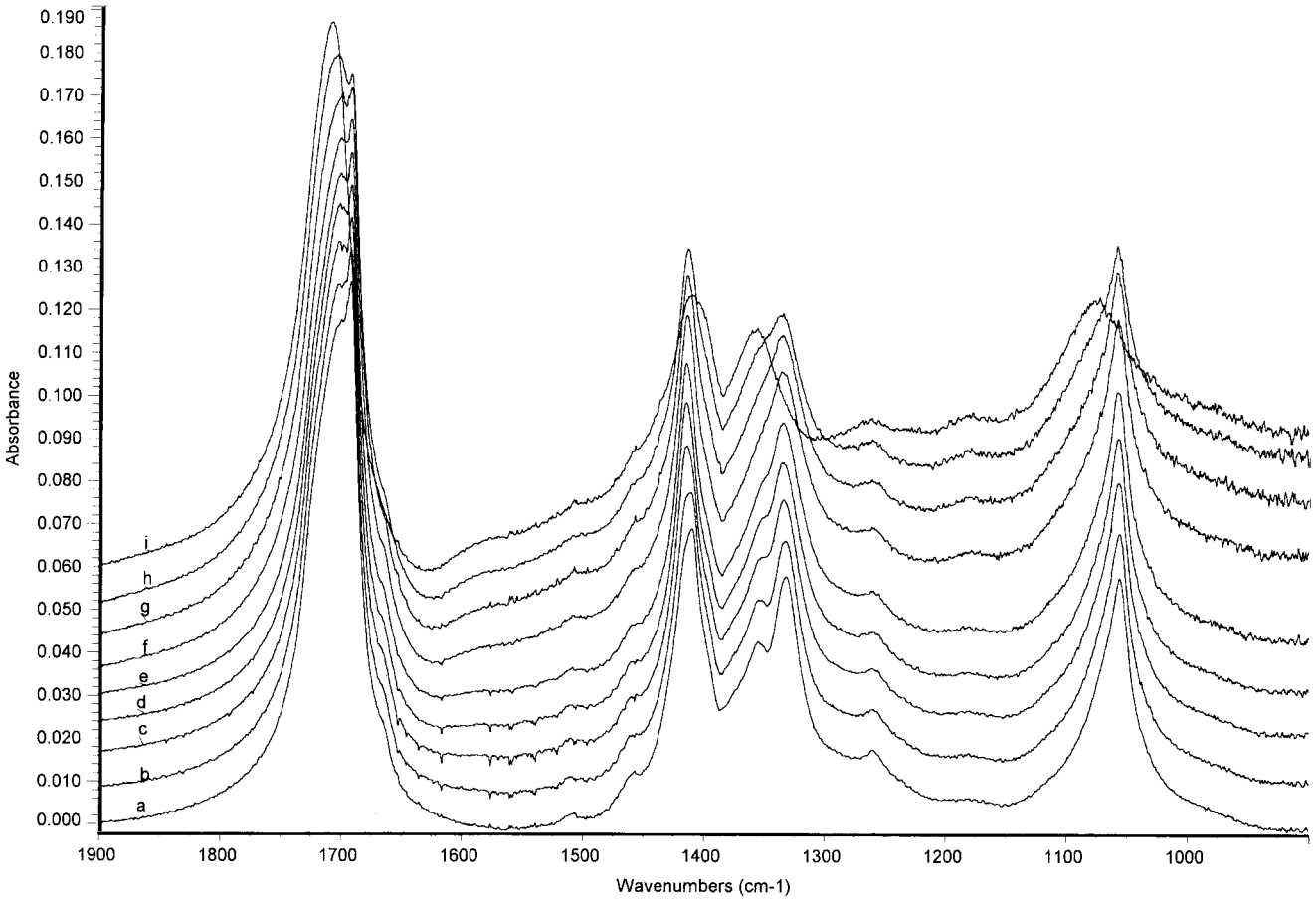

Fig. 8. Thermal history of a pristine Carilon sample (powder) followed by IR spectroscopy from $T = 28$ to 220°C. a: 28; b: 50; c: 70; d: 90; e: 120; f: 180; g: 200; h: 210; i: 220°C.

bands become sharp, but also C=O band undergoes a very relevant change of its shape with important intensity reduction of its broad high frequency components. These effects are practically absent in the case of the sample obtained from the surface on the back (Fig. 5(b)).

These observations suggest that during the photodegradation process a less stable, less dense, propylene rich, disordered phase is preferentially modified: in fact the drastic reduction of the asymmetric component observed in all the relevant IR transition indicates a remarkable reduction of a disordered, amorphous phase. Moreover, the disappearance of this "disordered phase" seems to occur as a consequence of the elimination of CH_3 units: indeed CH_3 band at 1459 cm^{-1} completely disappears in the exposed sample. This fact indicates that the photodegradation process takes place preferentially near the chemical defects (propylene units) along the polymer chains.

As a consequence of this process we expect that a large amount of short chains is formed. These short chains can eventually give rise to re-crystallisation in new highly ordered domains (probably in a crystalline phase similar to the α modification, which is the most stable in absence of propylene units). This idea is supported by the general aspect of the IR spectrum of the exposed sample: its spectrum has more symmetric and sharp bands, whose shapes are similar to those shown by the regularity bands of highly crystalline polymer sample [12,13]. Notice that the above conclusion is in agreement with the data from DSC measurements (see Section 5).

Moreover, the presence of C–O–C units reveals a possible mechanism of polymer degradation, discussed in Section 4.

3.3. Thermal treatment: infrared analysis

With the hope to carry out a direct comparison between the data collected from vibrational analysis and from DSC experiments we have studied the evolution of the IR spectra of two different sample of Carilon (a powder from pristine plate and a power scraped from the surface of the plate directly exposed for 7944 h.). The samples, as Kbr pellets, were heated in a Mettler hot stage FP800ht and the IR spectra were recorded at increasing values of the temperature (see Figs. 8 and 9).

Fig. 8 shows the temperature dependent spectra of Carilon. The sample was heated from 28 to 70°C and then cooled to 28°C. This allowed to verify that the (very little) changes

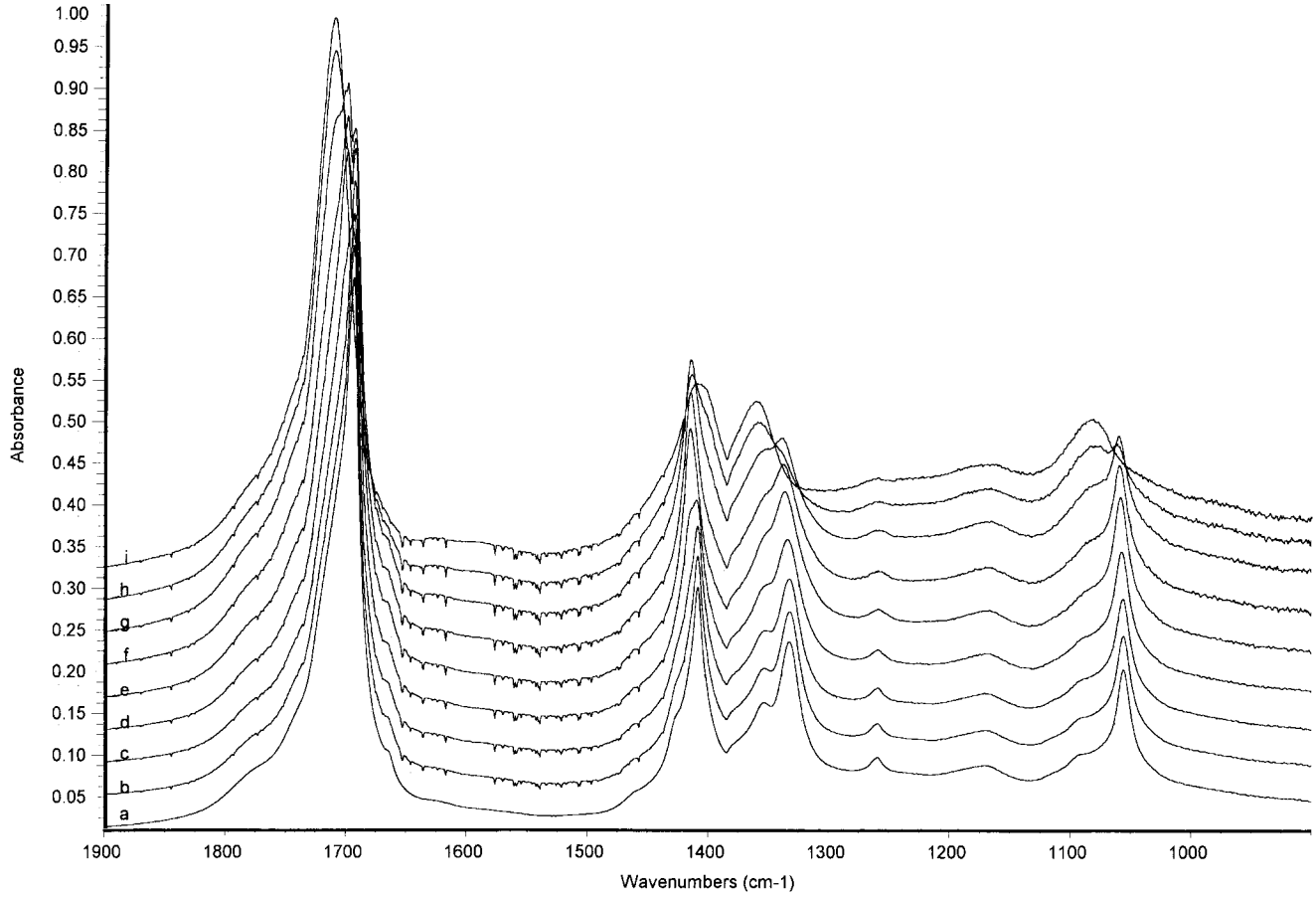

Fig. 9. Thermal history of a Carilon sample (powder) from the top surface of an exposed plate (7944 h of outdoor exposure) followed by IR spectroscopy from $T = 28$ to 200°C. a: 28; b: 50; c: 70; d: 90; e: 110; f: 140; g: 160; h: 180; i: 200°C.

observed are not reversible. Then the sample was heated from 28 to 220°C, where the melting is clearly observed.

During the whole thermal treatment only a few changes show up starting from 70°C. We observe small frequency shifts, which can be ascribed to some rearrangement of the crystalline phase, possibly a transition to the β form (more stable at high temperature) of the small amount of α crystalline domains which were present in the pristine sample.

Dramatic changes suddenly happen at 220°C, due to the melting of the sample. The frequencies of the fundamental bands of the molten sample are appreciably higher in frequencies with respect to the corresponding bands in the solid. This fact supports our assignment of the higher frequency components of the vibrational bands of the solid pristine sample to a conformationally disordered amorphous phase.

In Fig. 9 the thermal history of the photodegraded sample can be followed with IR experiments in a range of temperatures from 28 to 220°C. Comparison between the room temperature spectra of Figs. 9 and 10 (see also Fig. 5 spectra (a) and (c)) indicates that:

(i) From the view point of the crystal structure the photodegraded sample is mainly arranged in a well defined, highly crystalline phase, that is probably similar to the α phase described in Ref. [8] for the case of POK/C2. In fact IR bands are sharp; notice moreover, that peak frequencies are slightly lower than those of the pristine sample.
(ii) Due to the lack of propylene units after outdoor exposure, this α phase is made by short chains, originated by the breaking of the polymer chain during photodegradation.

According to what is reported in Ref. [8] on the effect of thermal treatment on POK/C2 we expect that at a given temperature crystals arranged in α phase rearrange in β phase (which is stable at higher temperature, i.e. 120°C for POK/C2). However, since photodegraded Carilon consists of a distribution of short chain lengths, we expect that $\alpha \rightarrow \beta$ transition does not occurs suddenly at a well defined temperature, but that it takes place over a wide range of temperatures according to the thermal stability of different α domains characterised by different chain lengths. For the same reason we also expect a lower melting temperature with respect to that of the pristine sample and a broad temperature range for melting.

The temperature dependent spectra of Fig. 9 support our expectation.

Spectra do not show changes up to 70°C: above this

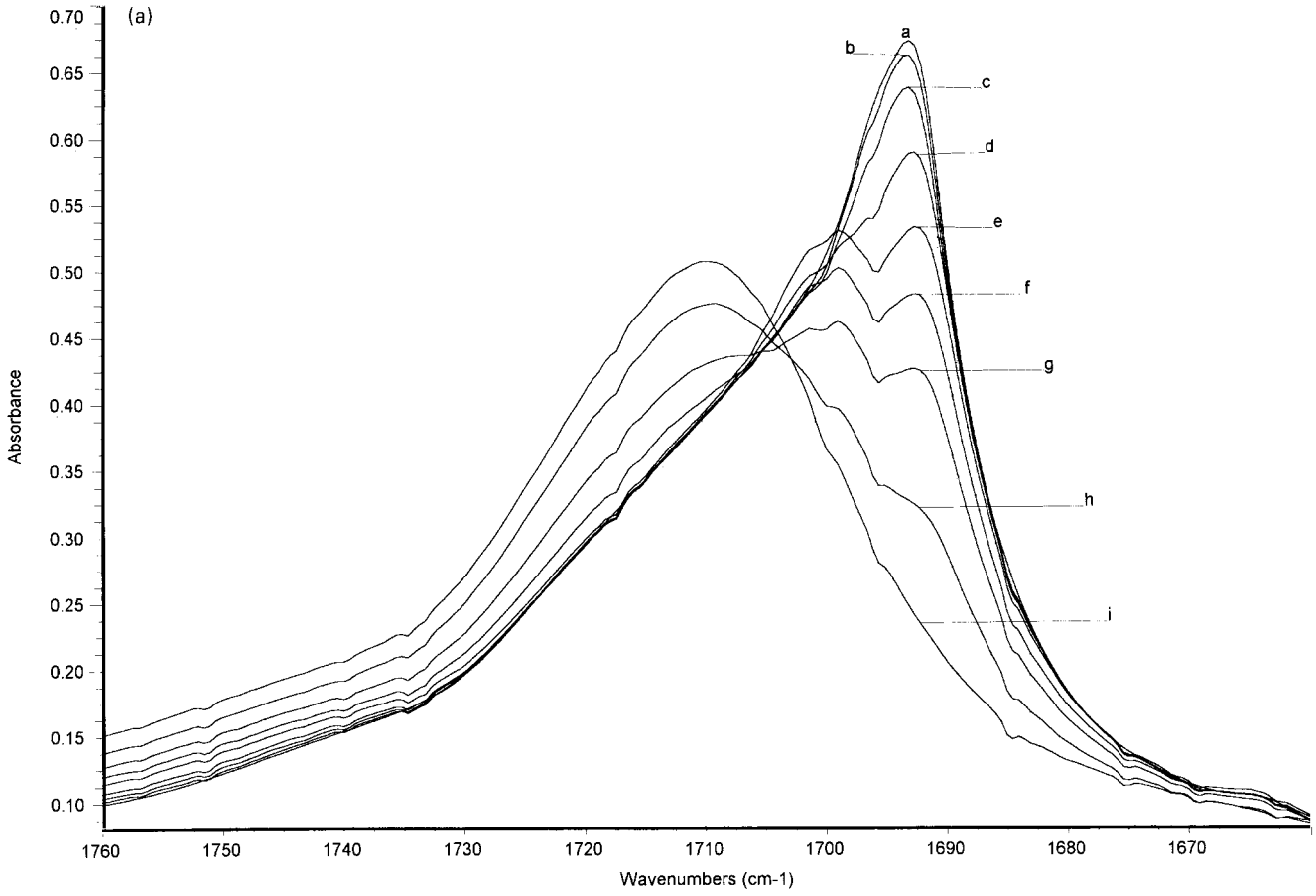

Fig. 10. Evolution of the IR spectrum of a photodegraded Carilon sample (7944 h of outdoor exposure) in a temperature range from $T = 28$ to 220°C. a: 28; b: 50; c: 70; d: 90; e: 120; f: 180; g: 200; h: 210; i: 220°C. (a) C=O stretching region; (b) CH_2 bending region. A common absorbance scale has been used to emphasise intensity changes of the different components (see text).

temperature a slow evolution of the fundamental bands starts (see Fig. 10(a) and (b)). A new component on the high frequency side of all relevant bands arises; simultaneously the intensity of the maximum peaks observed at room temperature decreases (for instance in the case of C=O stretching band we find a maximum at 1692 cm^{-1} at room temperature, at 70°C; a component at 1699 cm^{-1} appears; at 120°C the first component is strongly reduced and the peak shows only one maximum at 1699 cm^{-1} (see Fig. 10(a))). This spectral evolution can be related to a transition of crystalline domains from α to β phase. Melting starts at about 160°C, when a clear new component (centred at 1710 $cm^{-1)}$ arises on the high frequency side of C=O band; moreover, the appearance of the high frequency asymmetric components can be observed also for several other fundamental bands. With the increase of the temperature these asymmetric components develop into large bands with maximum frequency values equal to those observed in the molten pristine sample. At 180°C the whole crystalline domains of photodegraded sample are melt.

The fact that the IR experiments reveal a crystal-melt transition over a wide range of temperature can be correlated to the broad band observed with DSC experiments on plate surface directly exposed (see Section 5)

Moreover the indication of the presence of a α → β transition obtained with IR experiments can be related to a broad endothermic peak observed before the melting peak in DSC plots of the surface materials from photodegraded samples.

In conclusion, if we compare the thermal evolution of the pristine and photodegraded samples as seen by IR experiments, we have clear evidence of relevant rearrangements in the crystalline phase induced by outdoor ageing.

4. Photodegradation reactions

Degradation reaction could start with a photolysis of the carbonyl groups by the Norrish type I free radical process:

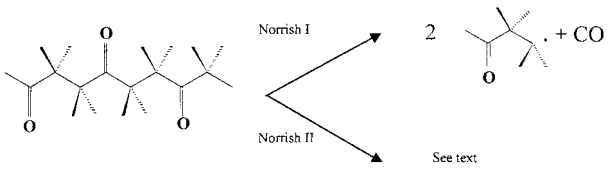

This reaction occurs with low quantum yield at wave

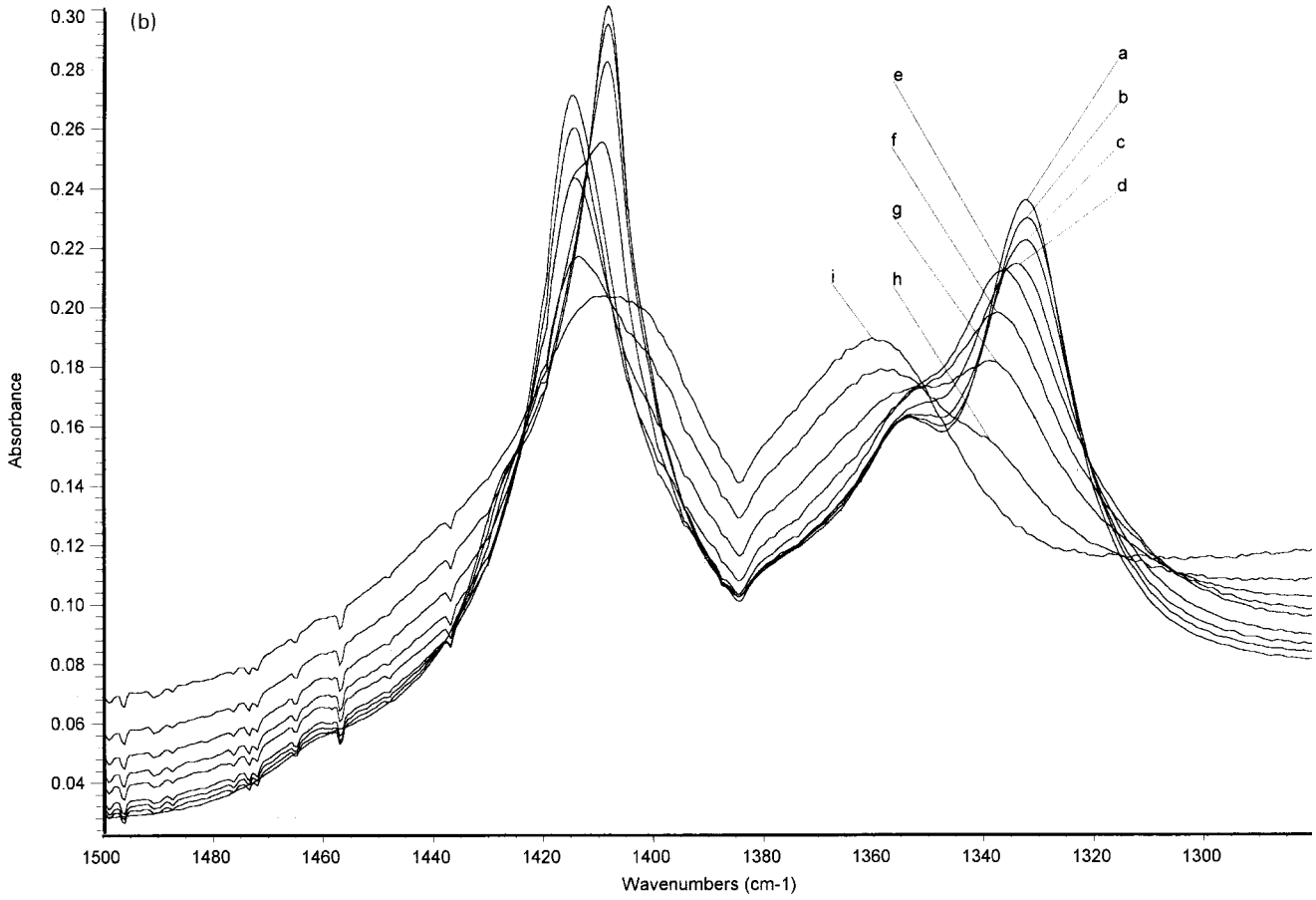

Fig. 10. (*continued*)

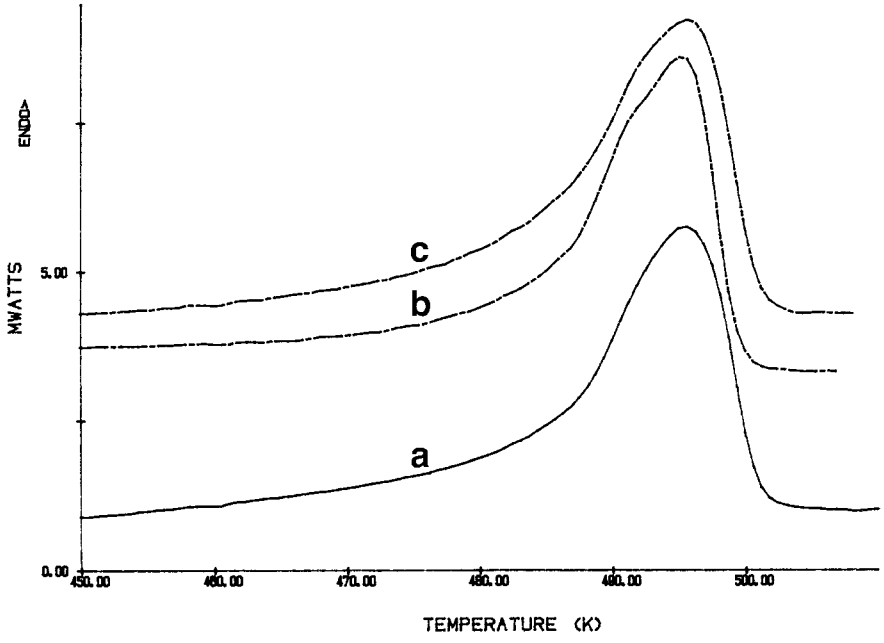

Fig. 11. DSC plot of bulk Carilon after different exposure times. Curve a: after 0 h; curve b: after 5112 h; curve c: after 7944 h.

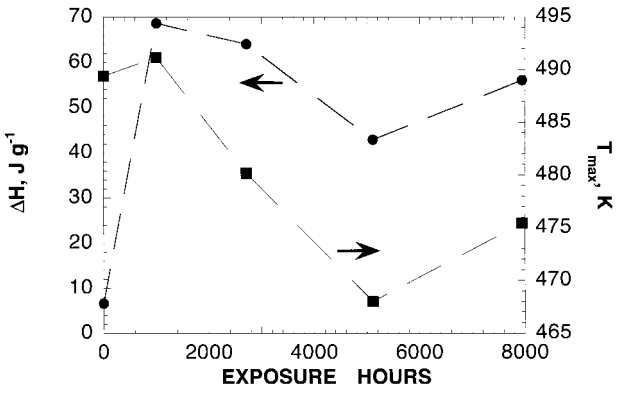

Fig. 12. Melting enthalpy and T_{max} (high temperature peak) of Carilon surface (powder scraped from the surface directly exposed, see text) as function of outdoor exposure times.

length emitted by sun and transmitted by the earth atmosphere [2]. Norrish type II reaction is practically inhibited due to the absence of hydrogen atoms in γ position to the carbonyl group [8]. In the presence of oxygen, free radicals produced by Norrish I can participate in photo-oxidation reactions which lead to photodegradation products. Degradation reactions could involve methylene groups adjacents to carbonyl and also *tert*-CH bonds present, at very low concentration, in the polymer. FT-IR spectra of photodegradation products show a structured band at 1161 cm^{-1}, attributable to C–O single bond. The appearance of these chemical groups cannot be directly explained according to the classical oxidation scheme.

Due to the chemical structure of the polymer a very strong carbonyl band dominates IR spectra of the pristine and of the photodegraded material. This band shows relevant changes that evolve during the exposure time. The interpretation of these changes, as proposed in this work, has been restricted to evidences of physical modifications of the material.

On the other hand, the carbonyl band observed has a very complicated structure and is certainly due to the envelope of several different components: for this reason other processes as for instance chemical modifications involving formation or disappearance of carbonyl bonds, that are probably involved in the photodegradation mechanism, cannot be clearly identified following the evolution of C=O stretching band.

5. Thermal analysis: differential scanning calorimetry and thermogravimetric analysis

DSC analysis of the unaged, bulk POK shows a single melting peak at 495 K (Fig. 11) with a ΔH_m of about 81 J/g. Lommerts et al. [8] report for the fully crystalline POK/C2 a ΔH_m in the range 215–330 J/g. On this basis a crystallinity value for our bulk material (before exposure) in the range 25–30% can be estimated.

In the bulk material, appearance of shoulders in the

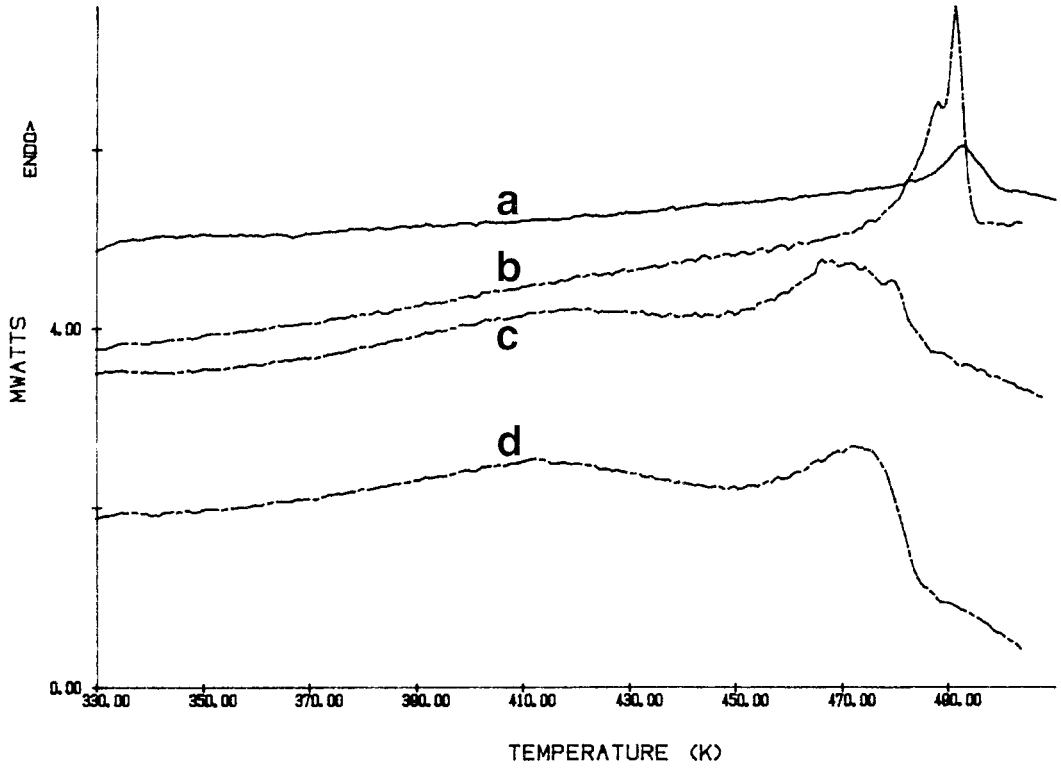

Fig. 13. DSC plot of Carilon surface (powder) after different outdoor exposure times. Curve a: 0 h; curve b: 1008 h; curve c: 5112 h; curve d: 7944 h.

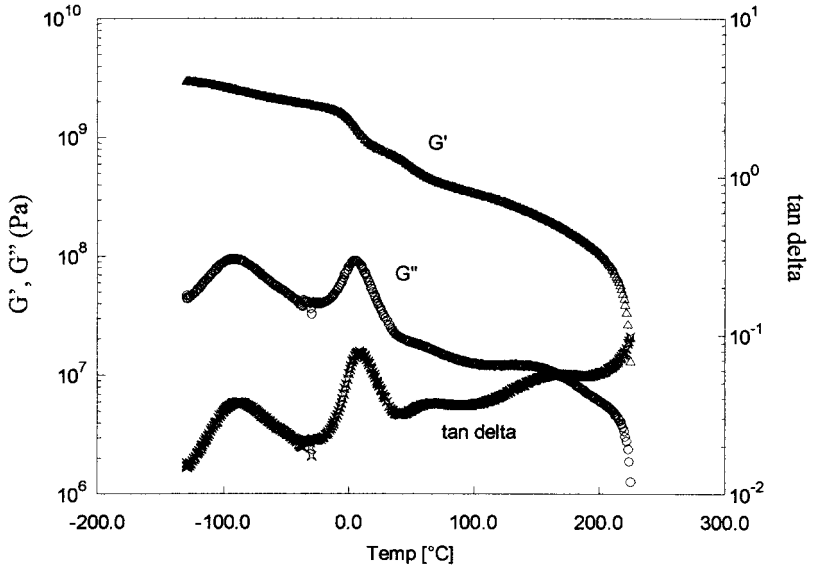

Fig. 14. Dynamic mechanical properties of Carilon.

melting peak was observed with increasing exposure times (see Fig. 11, where DSC plot at exposure time $t = 0$ h (curve a), $t = 5112$ h (curve b), $t = 7416$ h (curve c) are reported).

A marked difference is observed in the behaviour of the surfaces. The surfaces of the pristine sample exhibit a remarkably lower crystallinity compared to the pristine bulk material; both surfaces of the pristine samples are characterised by ΔH_m of about 6 J/g, while the peak T_m value remains practically unchanged (Fig. 12). This can be the result of a high temperature gradient at the polymer-mould interface consequent to relatively fast cooling during sheet moulding. The crystallinity of the material near to the exposed surface increases with exposure times: ΔH_m measured from a powder scraped from the surface directly exposed reaches a value beyond 60 J/g, i.e. beyond 70% the value of the bulk material already after 1000 h of outdoor exposure (Fig. 12).

The DSC traces of the surface material (obtained by scraping the plate surface directly exposed to the sun light) are remarkably different from those of the pristine polymer (see Fig. 13). After 1000 h of exposure the melting process clearly show new features, although the melting peak is still centred at the same temperature of the pristine material (about 490 K). After 5000 h of exposure (see Fig. 13) thermal analysis shows the appearance of two distinct endothermic effects, in the temperature ranges 355–440 and 445–485 K, respectively, i.e. well below the melting temperature of the pristine material. DSC experiments performed at lower scan rate (2.5 K/min) confirm the presence of two endothermic events. To explain the presence of the lower temperature endothermic event, the following hypothesis can be proposed: it can be the evidence of a solid $\alpha \rightarrow \beta$ transition in the partially degraded polymer, with very low propylene content. According to the results by IR analysis the degraded material has a high degree of crystallinity and is packed in α phase. Notice moreover, that a phase transition, ascribed to $\alpha \rightarrow \beta$ transition of the degraded material, has been seen by IR study of the thermal history of an exposed sample (see Section 3). Another possible explanation for the appearance of a low temperature endotherm is the occurrence of melting processes involving crystals formed by degradation products, with low melting point. Indeed, according to the IR spectra, new chemical species are formed, containing ether groups. The higher temperature peak should correspond to the onset of the melting of partially degraded Carilon chains. Above 470 K full degradation of the exposed material rapidly occurs.

The thermogravimetric analysis, in agreement with DSC results, shows a marked reduction of the oxidation strength of the surface material directly exposed to the light after more than 1000 h of exposure.

6. Mechanical tests

The dynamic mechanical analysis of Carilon shows the presence of different relaxation processes which occur in a wide temperature range. The plot of tan δ as function of temperature (Fig. 14) of the unaged material shows a main damping peak centred at about 15°C which indicates the activation of collective chain motions in the amorphous phase and is attributed to the glass transition. In this temperature range a variation of stiffness of about 50% (G') is observed. A secondary, broad relaxation process with lower activation energy is evidenced at about −90°C, which indicates the possibility of localised motions of chain segments. A similar peak, centred at about −120°C, is found for high density polyethylene, which was attributed to torsional motions of short segments of the polymer chain [15]. Due to the structural similarities between linear polyethylene and polyoxyketone (POK), it is reasonable to think

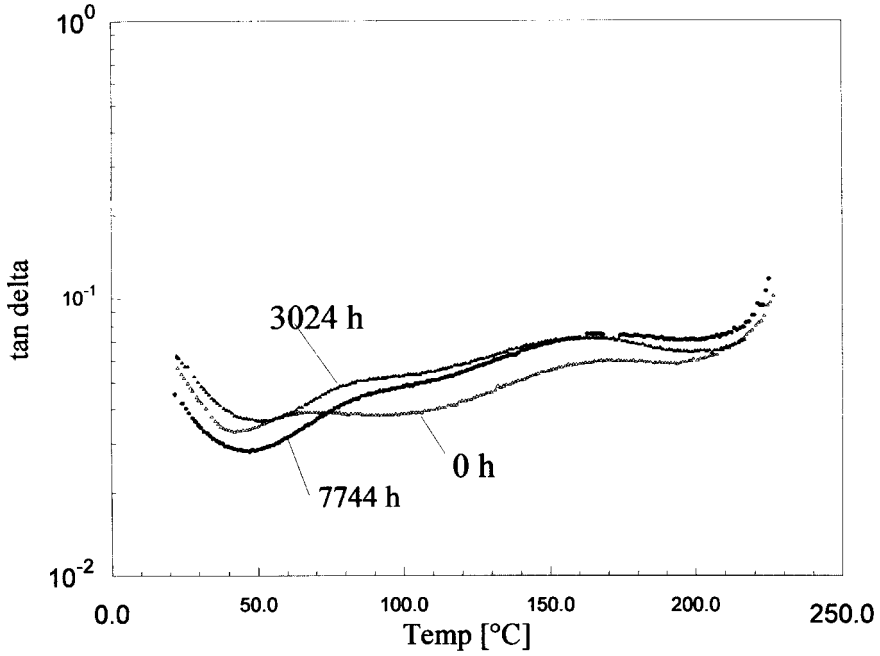

Fig. 15. The tan δ as function of temperature of Carilon after different ageing times.

that a similar relaxation mechanism takes place also in Carilon, in nearby temperature ranges. The torsional flexibility of POK units, however, may be reduced with respect to that of polyethylene, due to the presence of C = O bonds: this fact may explain the higher peak temperature observed in Carilon samples.

Relaxation processes at temperatures higher than T_g are observed at about 70 and 160°C. Since they occur above the T_g, these processes should be related to the activation of some motions involving chains in the crystalline phase. Klop et al. reported evidence of a partially reversible transition between α and β crystalline forms occurring in oriented, pure POK in this temperature range, depending on the molecular weight and thermal history [8]. Notice that the IR spectra (Section 3) also show some little rearrangement of the crystalline phase at 70°C. At about 220°C the material melts and the tests were stopped.

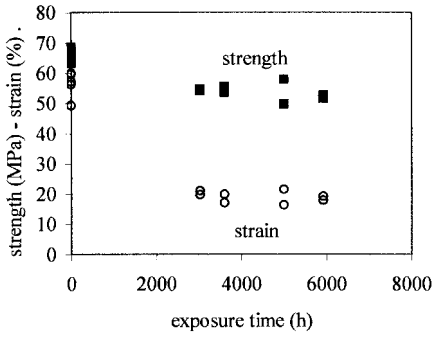

Fig. 16. Strength and strain at breaking data of Carilon after different ageing times.

The analysis of Carilon samples after different outdoor ageing times does not show marked changes in the dynamic mechanical behaviour; the positions of the glass transition and of the low temperature secondary transition remain unchanged. However, the relaxation process centred at about 70°C in the pristine material, shifts to higher temperatures with increasing the exposure time, progressively merging into the broader peak, which remains fixed and centred at about 160°C (Fig. 15).

Tensile tests performed on Carilon samples after different exposure times show a marked influence of ageing. It was observed that, while the strength is little affected by the ageing, the elongation at break remarkably decreases, already after 3000 h of exposure (Fig. 16). The unaged material, exhibits a yield point followed by extensive necking during tension, with elongation exceeding 50%. The same behaviour is observed for a pristine Carilon sample after annealing treatment at 80 or 180°C for 3 h.

In the aged material, although the deformation behaviour before the yield point is little affected, no necking is observed and the material breaks at remarkably lower strains (Fig. 17). Samples aged at times longer than 3000 h do not show further difference in the stress/strain plots.

While spectroscopic techniques and thermal analysis show that photodegradation is very effective in a thin layer of material near to the surface directly exposed to the sun light and do not identify modifications involving the bulk materials, mechanical test suggests that outdoor ageing do involve, in some extent, the whole sample.

On the other hand, the brittle behaviour observed for the aged samples could be justified also in the absence of polymer degradation in the bulk, if some crazes confined in a

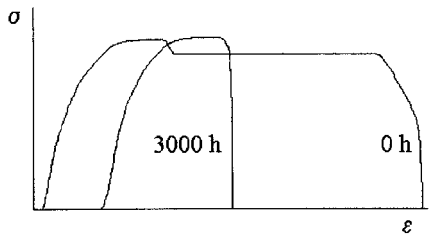

Fig. 17. Comparison of outdoor aged and pristine Carilon stress–strain curves.

thin layer near to the exposed surface (see in Section 7 evidences from SEM experiments) propagate under the action of the applied stress.

In order to check the above hypothesis, tensile tests were performed on exposed samples (6744 h) after removal of a surface layer of more than 100 μm: no appreciable difference in the break strain and strength was observed compared to the other aged samples. This suggests that effects of polymer degradation may not be confined on the surface: the embrittlement of the bulk material should be necessarily ascribed to changes of polymer structure, resulting from physical ageing, possibly assisted by photodegradation.

These modifications may be of the same nature as those identified by IR and DSC analysis on the exposed surface, which progressively involve the bulk material. The concentration of modified chains in the bulk material should be, however, very low, since they cannot be detected with spectroscopic techniques. On the other hand, it should be considered that even a small amount of short chains originated by photodegradation may remarkably reduce the material extensibility.

A similar behaviour was found in the case of oxidation of polypropylene assisted by sunlight exposure [16]. In this case also, photo-oxidation is mainly induces surface cracking; however, the bulk material show loss of mechanical properties, already at very low levels of chemical reaction.

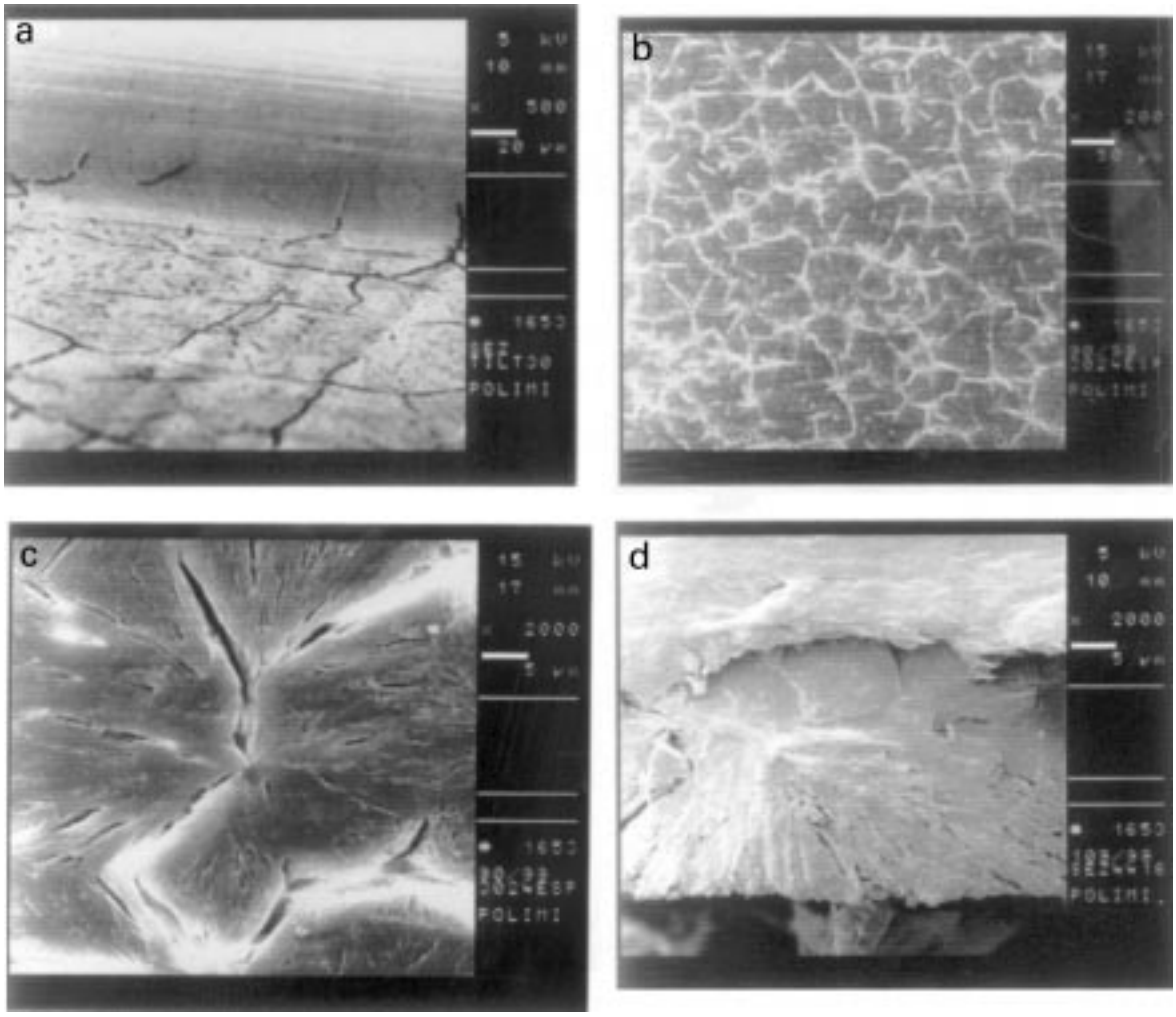

Fig. 18. SEM micrographs of Carilon surface after different exposure times: (a)500 h — 500×; (b) 3000 h — 200×; (c) 3000 h — 2000×; (d) 4400 h, cross-section, 2000×.

7. Scanning electron microscopy analysis

The surface morphology of POK plates after different exposure times was observed at SEM. The bottom surface did not show marked morphological changes even after more than 4400 h of exposure. On the contrary the exposed surface, already after 500 h of exposure, showed surface cracks forming a network through the samples (Fig. 18).

Observations of sample sections after increasing ageing times indicated that such cracks have a maximum depth of about 40 μm, which does not seem to increase with exposure time. The observation of such surface cracks indicate that they depart in a radial fashion which remind a spherulitic morphology. A relation between the cracks and the crystalline nature of the material could not, however, be established.

8. Conclusions

Carilon photodegradation takes place when the polymer is outdoor exposed. FT-IR absorption spectra, and ATR FT-IR spectra of exposed Carilon plates indicate that a photodegradation process takes place, involving the formation of C–O–C groups and that the process is accompanied by the disappearance of methyl units.

The highly degraded phase is certainly confined in a thin layer of material near to the exposed surface, as directly proven by DSC experiments on powder obtained by scraped surfaces and also by SEM images on thin films and plates of exposed Carilon samples.

The general aspect of the IR spectra indicate that, as a consequence of photodegradation, the more disordered phase is removed and/or reorganised: modified surfaces with an enhanced percentage of the crystallinity degree are indeed created. For this reason we expect an enbrittlement of the material near the exposed surface due to the lack of a 'plastic matrix' between crystalline hard domains.

IR analysis performed during thermal treatment of pristine and photodegraded samples show that the nature of the crystalline phase in the two samples is very different and strongly support the hypothesis of chains breaking and crystal rearrangement during outdoor exposure.

At difference from the data collected from IR, DSC and SEM analysis, which reveal relevant modifications of the material, localised near to the exposed surface, mechanical tests show properties variations which involve the whole, bulk material. Indeed, tensile tests performed on exposed Carilon samples show a remarkable loss of plastic deformation. This indicates that modification induced by the outdoor exposure could involve also the bulk material. The fact that no bulk modifications are identified by IR, DSC and SEM experiments suggests that already at very low concentration of photodegraded chains, the material looses its mechanical properties.

A similar behaviour has been reported in the case of the oxidation of polypropylene exposed outdoor [16].

Acknowledgements

The help of M. Pardi and M.R. Pagano in performing the SEM analysis and the mechanical tests is gratefully acknowledged.

References

[1] Carilon. Technical Publication. SHELL CHEMICALS, 1999.
[2] Hartley GH, Guillet JE. Macromolecules 1968;1:165.
[3] Gooden R, Davis DD, Hellman MY, Lovinger AJ, Winslow FH. Macromolecules 1988;21:1212.
[4] Mark HF, Bikales NM, Overberger CG, Menges G. Encyclopedia of polymer science and engineering. 2nd ed., vol. 10. New York: Wiley Interscience, 1985, p. 372.
[5] Severini F, Gallo R, Brambilla L, Castiglioni C, Ipsale S. J Polym Degrad Stab 2000;69:133.
[6] Data from U.C.E.A. Banca Dati Agrometeorologica Nazionale, www.inea.it/ucea/uceaind.htm.
[7] Klop EA, Lommerts BJ, Veurink J, Aerts J, Van Puijenbroek RR. J Polym Sci, Polym Phys Ed 1995;33:315.
[8] Lommerts BJ, Klop EA, Aerts J. J Polym Sci, Polym Phys Ed 1993;31:1319.
[9] Donald HP, Ward S. Polymer 1961;2:341.
[10] Snyder DJ, Schachtschneider JH. Spectrochim Acta 1964;20:853.
[11] Lagaron JM, Powell AK, Davidson NS. Macromolecules 2000;33:1030.
[12] Painter PC, Coleman MM, Koenig JL. The theory of vibrational spectroscopy and its applications to polymeric materials. New York: Wiley, 1982.
[13] Zerbi G. In: Advances in infrared and Raman spectroscopy. Clark RJH, Hester RE, editors. London: Heyden, 1984, p. 301.
[14] Duncan ABF, Matsen FA, Gordy W, Sandorfy C, Jones RN, West W. Chemical applications of spectroscopy. West W, editor. New York: Interscience, 1956.
[15] Billmeyer FW. Textbook of polymer science. New York: Wiley, 1971, p. 211.
[16] Billingham NC. Makromol Chem, Macromol Symp 1989;28:145.